Coordination Solids via Assembly of Adaptable Components: Systematic Structural Variation in Alkaline Earth Organosulfonate Networks

Adrien P. Côté and George K. H. Shimizu*[a]

Abstract: A family of alkaline earth organosulfonate coordination solids is reported. In contrast to more typical crystal engineering approaches, these solids are sustained by the assembly of building blocks that are coordinatively adaptable rather than rigid in their bonding preferences. The ligand, 4,5-dihydroxybenzene-1,3-disulfonate, L, progressively evolves from a 0D, 1D, 2D, to a 3D microporous network with the Group II cations Mg^{2+}, Ca^{2+}, Sr^{2+}, and Ba^{2+}, (compounds **1**–**4**), respectively. This trend in dimensionality can be explained by considering factors such as hard–soft acid–base principles and cation radii, a rationalization which follows salient crystal engineering principles. The selective gas sorption properties of the microporous 3D network [Ba(L)-(H_2O)]·H_2O, **4**, with different gaseous guests are also presented.

Keywords: alkaline earth metals · coordination complexes · crystal engineering · host–guest systems · sulfonate ligands

Introduction

The identification and development of novel solid-state architectures is a general theme in the pursuit of new functional materials. A major goal is to derive relationships between a solid's structure and its properties and then use these correlations to design new materials. However, at times, finding strategies to prepare a designed solid-state architecture can be highly empirical, and obtaining a phase with the desired organization of components becomes a trial and error process. Thus, there is an inherent value to forming a pool of information from the a posteriori structural rationalization of compounds from which a set of principles can be extracted to allow future structures to be predicted. The first approach is to identify trends within a narrow set of parameters, for example, by systematically changing the nature of one component in a solid-state compound.

A promising method to prepare designed solid-state materials is to employ organic ligands and metal ions as building blocks.[1] By taking into account the coordination modes and ligating preferences of metal cations and bridging ligands, the concepts of crystal engineering of coordination solids have evolved over recent years.[2] In efficiently designed metal-polycarboxylates and -polypyridines, often predictions can be made based upon the usual coordination geometry of the chosen metal center and the denticity and shape of the ligand.[3] Crystal engineering descriptors such as "net topologies" with associations made to atomic network solid structures have evolved a means to categorize coordination solids and as design starting points for preparing extended networks.[4]

The vast majority of work on coordination solids concerns transition metals, however, s-block metals have received relatively little attention.[5] From a synthetic standpoint, transition-metal cations as tectons are more natural choices owing to the well-defined coordination geometries of d-block cations and cation clusters. Comparatively, aversions to using s-block cations as building blocks arise from their unpredictable coordination numbers and geometries as no ligand field stabilization effects govern their bonding.[6] The observed coordination trends in s-block chemistry are better correlated with the less exacting parameters of cation radius and charge density. Another issue for framework assembly with s-block ions is their high affinity for oxygen donors, particularly water. This tendency to form solvated metal centers upon crystallization inhibits the metal-ligand cross-linking required to form an extended structure. Given the less predictable nature of s-block assemblies, it seems counter-intuitive to use them as building blocks for coordination solids. However, less structural predictability does not preclude high degrees of order nor functionality, as will be shown in this work.

Research in our group is focussing on the use of organosulfonates (RSO_3^-). Sulfonates are structurally analogous to organophosphonates (RPO_3^{2-}), another class of ligands

[a] Prof. G. K. H. Shimizu, A. P. Côté
Department of Chemistry, University of Calgary
2500 University Drive N.W.
Calgary, Alberta, T2N 1N4 (Canada)
Fax: (+1) 403-289-9488
E-mail: gshimizu@ucalgary.ca

Supporting information for this article is available on the WWW under http://www.chemeurj.org or from the author.

 DOI: 10.1002/chem.200305102

successfully used for the formation of functional coordination solids.[7] Similarly with the other types of ligands previously discussed, phosphonates strongly bind to transition metals and are valued because they very predictably form layered networks with a well-defined mode of connectivity between ligands and metal ions. In comparison, sulfonates have less ligating ability due to their lowered anionic charge, and are broadly classified as soft and weakly coordinating. So, upon aqueous complexation with harder transition-metal cations, sulfonates tend to form hydrated compounds, with the sulfonate groups forming hydrogen bonds to the aquo ligands (i.e., second-sphere complexes).[8] When softer cations, such as 3rd–5th row alkali or alkaline earth are employed, direct coordination of sulfonate ligands can be enabled. With appropriate ligands, this can result in cross-linking between metal centers to form network structures,[9–11] even when crystallized from water. Within these networks it is observed that -SO_3 groups can achieve every possible mode of bridging (Figure 1). The observation that sulfonates have a wide range of bonding modes in these structures has led us to describe the group as a "ball of Velcro".[9a, 12]

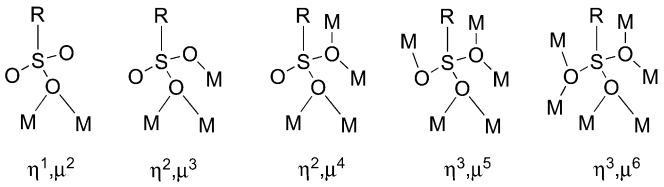

Figure 1. Observed coordination modes for sulfonate ions.

Our approach towards the preparation of new coordination networks uses a less rigorous adherence to current crystal engineering concepts: If one employs a ligand with weaker, more variable coordinative tendencies, in our case organosulfonates (RSO_3^-), in conjunction with metals ions with pliant coordination spheres, such as s-block cations, the energetic minimum to form the most stable network becomes more accessible because both the metal and ligand are coordinatively adaptable.[13] This strategy follows hallmark supramolecular concepts in that multiple weak interactions are being employed cooperatively to ultimately form stable structures.[14] In this sense, transition metal polycarboxylate, -polypyridyl, and -phosphonate coordination networks may be regarded as being engineered from the "rigid–rigid" association of highly preorganized building blocks. s-Block metal–sulfonate networks result from the assembly of coordinatively adaptable metal and ligand building blocks.

Herein, we have studied the coordination chemistry of the disulfonated catechol, 4,5-dihydroxybenzene-1,3-disulfonate, L, with alkaline earth cations. L forms more aggregated structures with higher Group II cations, progressively forming a 0D solvent separated structure with Mg^{2+} (**1**), 1D columnar structure with Ca^{2+} (**2**), 2D layered structure with Sr^{2+} (**3**), to finally a 3D microporous coordination framework with Ba^{2+} (**4**). In previous studies with disulfonated ligands and Group II cations, it has been generally observed that lamellar networks are formed.[15–16] Significantly, $[Ba(L)(H_2O)]\cdot H_2O$, **4**, is a robust network, stable to $>400\,^{\circ}C$, which possesses selective and reversible gas sorption properties.[17] These different structural trends can be correlated with cation radius, which directly affects chemical softness and coordination number. Moreover, this work shows that, from coordinatively adaptable building blocks, stable and functional solids are attainable.

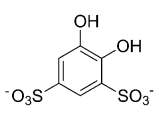

L

Results and Discussion

Single crystal structures: Single crystal structures were obtained as hydrates for all the alkaline earth salts of L. For the sake of visualization, Figures 2–5 are presented as an initial view of the overall structures of **1**–**4**, respectively. Each compound is discussed in more detail. The Mg^{2+} structure, **1**,

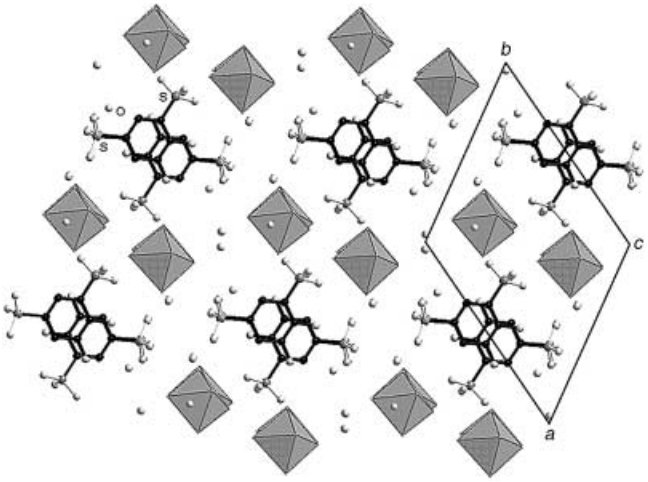

Figure 2. Packing arrangement of $[Mg(H_2O)_6]\cdot L\cdot 3H_2O$, **1**, viewed along the crystallographic *c* axis showing the solvent separated arrangement of the structure provided by the coordinated and included H_2O. $Mg(H_2O)_6^{2+}$ centers are represented by polyhedra.

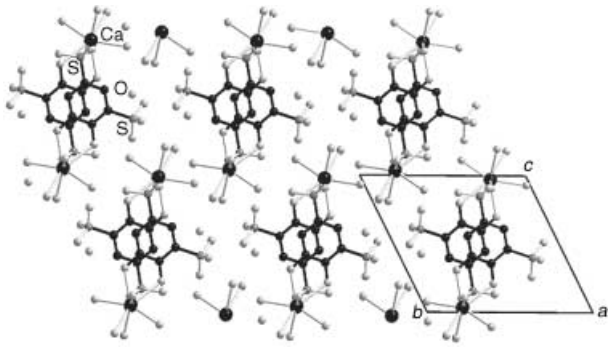

Figure 3. View onto the 1D columns in $[Ca(L)(H_2O)_4]\cdot H_2O$, **2**, which run parallel to the *a* axis.

can be classified as a 0D network and is a solvent separated ion-pair solid (Figure 2). However, the Ca^{2+}, **2**, Sr^{2+}, **3**, and Ba^{2+}, **4**, salts form extended coordination networks through both bonding to the catechol moiety and the -SO_3 groups of L. An increasing degree of aggregation is observed between

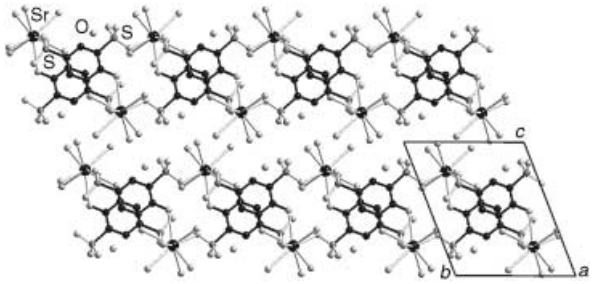

Figure 4. Layered 2D structure of $[Sr(L)(H_2O)_4]\cdot H_2O$, **3**, viewed along the crystallographic *a* axis. Lamella lie parallel to the *ab* plane with the included and coordinated water molecules projecting into the interlayer region.

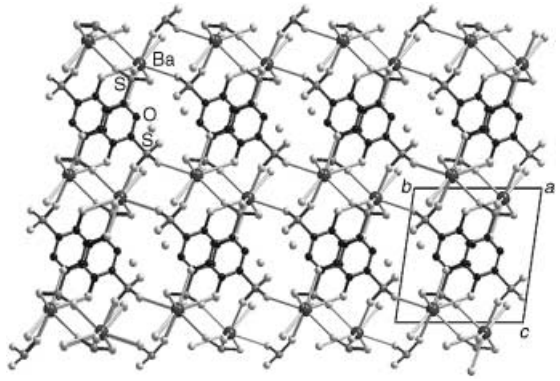

Figure 5. 3D pillared layered structure of $[Ba(L)(H_2O)]\cdot H_2O$, **4**, viewed along the *a* axis. The water filled ~4 Å channels lie between molecules of L in the interlayer region which support the 2D $[BaSO_3]_\infty$ aggregation in the *ab* plane.

ligands and metals in **2**–**4** resulting in a 1D columnar motif for Ca^{2+} (Figure 3), 2D lamellar structure for Sr^{2+} (Figure 4), to a 3D pillared layered structure for Ba^{2+} (Figure 5). This increase in dimensionality stems from the larger radii and polarizability of heavier M^{2+} ions, and the resulting compatibility with soft sulfonate anions. A parallel trend is the lowered affinity for the softer cations to coordinate to water molecules, allowing for more cross-linking. The structural unit $M^{2+}L$, where the catechol (4,5-diol) moiety of L chelates the metal center in a doubly protonated form, can be viewed as a synthon in these networks, as, undoubtedly, this strongly ligated unit would form first.[18] More detailed features of **2**–**4** are illustrated in the asymmetric units presented in Figure 6a–c discussed below. Details of the single crystal X-ray analyses are given in Table 1.

$[Mg(H_2O)_6]\cdot L\cdot 3H_2O$ (1): This structure is an example of a purely second sphere network as the catechol moiety of L does not coordinate to Mg^{2+} (Figure 2). Mg^{2+} is present as a hexaaquo species and forms charge assisted hydrogen bonds with sulfonate ligands, typical of Mg^{2+} sulfonate salts.[19] Overall, the extended structure can be perceived as having a layered motif with hexaaquo Mg centers and interstitial water molecules alternating with sheets of L. There are two crystallographically distinct molecules of L that exist as a π-stacked pair (3.2 Å) in the asymmetric unit. This dimer further π-stacks (3.3 Å) with neighboring pairs of L along the *z* direction. The sulfonate groups form hydrogen bonds to $[Mg(H_2O)_6]^{2+}$ centers (Figure 7). The number of hydrogen-bonding contacts between sulfonate oxygens and coordinated water molecules ranges from two to five for each SO_3 group (D···A 2.72–2.91 Å).[20] All Mg–O bond lengths and angles are within normal limits ranging 2.027(2) to 2.134(2) Å.

$[Ca(L)(H_2O)_4]\cdot H_2O$ (2): The building block for this structure (as well as **3** and **4**) can be viewed as 1:1 M:L complex where L chelates to Ca^{2+} via the catechol moiety (O7–Ca1 2.579(2), O8–Ca1 2.508(2) Å). The columnar motif observed in this network originates from a 1D aggregation of these chelated CaL units via sulfonate ligation (Figure 3). Only one CaL unit present is in the asymmetric unit. These units link along the *z* direction to give a 1D chain (Figure 8). Each CaL unit is joined to the next via the sulfonate group in the 1-position to bridge metal centers in an η^2,μ^2-coordination mode (O1–Ca1 2.358(2) Å, O2–Ca1 2.395(2) Å), leaving the second sulfonate group uncoordinated. The coordination spheres are completed to 8-coordination by bridging sulfonate groups and four

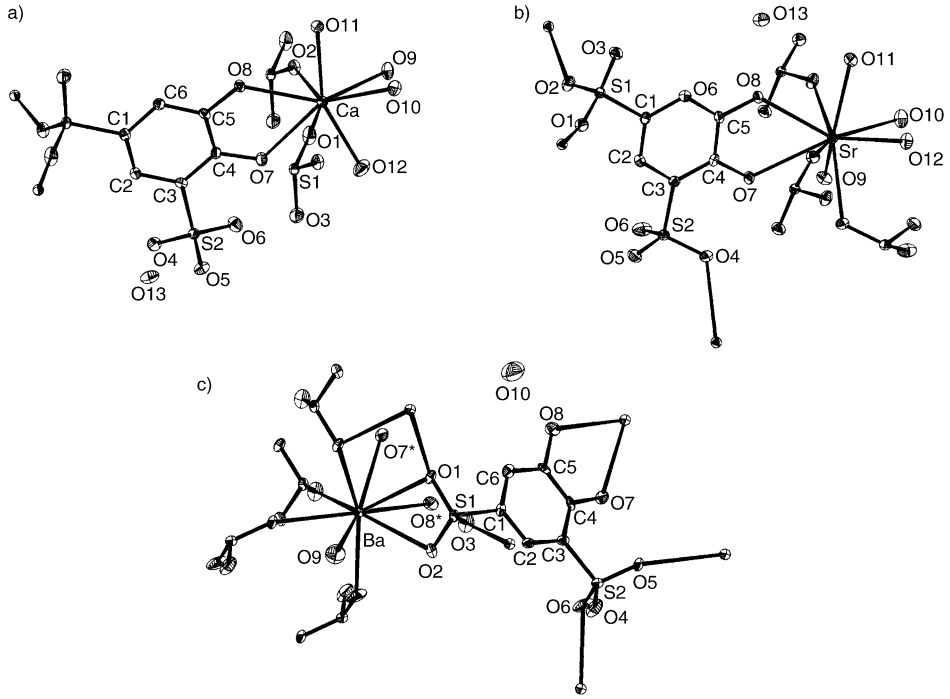

Figure 6. Elaborated asymmetric units for a) $[Ca(L)(H_2O)_4]\cdot H_2O$, b) $[Sr(L)(H_2O)_4]\cdot H_2O$, c) $[Ba(L)(H_2O)]\cdot H_2O$ in ORTEP representation. Note the increased number for metal–sulfonate contacts going from Ca^{2+} to Ba^{2+}. Ellipsoids are displayed at 50% probability.

Table 1. Crystal data and refinement summaries for $[Mg(H_2O)_6]\cdot L\cdot 3H_2O$, $[Ca(L)(H_2O)_4]\cdot H_2O$, $[Sr(L)(H_2O)_4]\cdot H_2O$, and $[Ba(L)(H_2O)]\cdot H_2O$.

	$[Mg(H_2O)_6]\cdot L\cdot 3H_2O$ $C_{12}H_8O_{34}S_4Mg_2$	$[Ca(L)(H_2O)_4]\cdot H_2O$ $C_6H_{14}O_{13}S_2Ca$	$[Sr(L)(H_2O)_4]\cdot H_2O$ $C_6H_{14}O_{13}S_2Sr$	$[Ba(L)(H_2O)]\cdot H_2O$ $C_6H_8O_{10}S_2Ba$
F_w	873.04	398.37	445.91	441.58
cryst. system	triclinic	triclinic	triclinic	triclinic
space group	$P\bar{1}$ (no.2)	$P\bar{1}$ (no.2)	$P\bar{1}$ (no.2)	$P\bar{1}$ (no.2)
a [Å]	12.6470(2)	6.9670(1)	7.1504(4)	7.3374(6)
b [Å]	13.5720(2)	10.1960(1)	9.4068(5)	8.6976(7)
c [Å]	13.6570(2)	11.0340(2)	11.2044(6)	9.2006(8)
α [°]	98.0670(9)	63.3090(7)	68.005(1)	81.923(2)
β [°]	108.111(1)	84.6170(7)	83.4916(9)	89.367(2)
γ [°]	117.0071(8)	85.978(1)	81.708(1)	84.313(2)
V [Å^3]	1872.21(5)	696.85(2)	690.01(6)	578.74(8)
Z	2	2	2	2
ρ_{calcd} [g cm^{-3}]	1.549	1.899	2.146	2.535
μ [mm^{-1}]	0.396	0.819	4.279	3.842
λ [Å]	0.71073	0.71073	0.71073	0.71073
R_f (sig reflns)[a]	0.050	0.027	0.026	0.028
Rw (sig reflns)[b]	0.153	0.085	0.067	0.067

[a] $R_f = (\Sigma(F_o - F_c)/\Sigma(F_o)$. [b] $R_w = (\Sigma w(F_o - F_c)^2/\Sigma w(F_o)^2)^{0.5}$.

Figure 7. Hydrogen bonding network and π-stacking observed between molecules of L in $[Mg(H_2O)_6]\cdot L\cdot 3H_2O$. Hydrogen bonding with included water molecules has been omitted for clarity.

aquo ligands. The 1D $[CaL(H_2O)_4]_8$ assemblies connect through hydrogen bonding between coordinated water molecules of adjacent columns (D···A: O9···O11 2.912(3) Å, O11···O10 2.808(3) Å), and coordinated water molecules and sulfonate groups (D···A 2.705(3) – 3.182(3) Å). From the distance between inter-column Ca^{2+} centers, the $[CaL]_\infty$ columnar aggregates are separated by 11.03 Å in the y direction, and 10.20 Å in the z direction. A molecule of water is bordered by the uncoordinated sulfonate groups, and is held by four hydrogen bonds (D···A 2.604(3) – 3.043 Å).

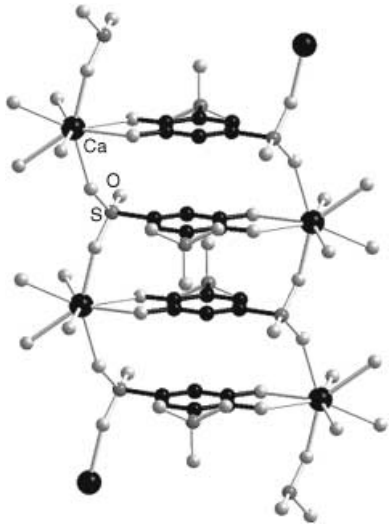

Figure 8. The 1D column formed in $[Ca(L)(H_2O)_4]\cdot H_2O$.

Table 2. Selected bond lengths [Å], angles [°] and torsion plane angles [°] for $[Ca(L)(H_2O)_4]\cdot H_2O$.

Ca1–O1	2.358(2)
Ca1–O7	2.579(2)
Ca1–O9	2.502(2)
Ca1–O11	2.415(2)
Ca1–O2	2.395(2)
Ca1–O8	2.5081(2)
Ca1–O10	2.558(2)
Ca1–O12	2.339(2)
O1-Ca1-O2	150.62(7)
S1-O2-Ca1a	146.09(1)
C5-O8-Ca1	124.13(2)
S1-O1-Ca1	157.95(2)
C4-O7-Ca1	121.43(2)
O7-Ca1-O8	61.79(6)
C5-C4-O7-Ca1	0.2(3)
O8-Ca1-O7-C4	– 0.35(2)
C4-C5-O8-Ca1	– 0.6(3)
O7-Ca1-O8-C5	0.49(2)

[a] The equivalent positions for $P\bar{1}$ are 1) x,y,z and 2) $-x,-y,-z$.

$[Sr(L)(H_2O)_4]\cdot H_2O$ (3): The Sr^{2+} layered structure (Figure 4) can be regarded as a further aggregated version of the Ca^{2+} network. In **3**, core catechol bound SrL units are again observed (O7–Sr1 2.813(2) Å, O8–Sr1 2.693(2) Å) which link into a similar columnar motif, as in **2**, via a sulfonate group (O1–Sr1 2.534(2) Å, O2–Sr1 2.570(2) Å). However, the second sulfonate group, previously uncoordinated, now penetrates the cation's coordination sphere in a monodentate fashion (O4–Sr1 2.675(3) Å), to crosslink the columns. This forms a two-dimensional motif and makes the coordination number of Sr^{2+} nine versus eight for Ca^{2+}, still with four aquo

Table 3. Selected bond lengths [Å], angles [°] and torsion plane angles [°] for $[Sr(L)(H_2O)_4]\cdot H_2O$.

Sr1–O1	2.534(2)
Sr1–O4a	2.675(2)
Sr1–O8	2.693(2)
Sr1–O10	2.696(2)
Sr1–O12	2.5721(2)
Sr1a–O2	2.534(2)
Sr1–O7	2.813(2)
Sr1–O9	2.614(2)
Sr1–O11	2.678(2)
O1-Sr1-O2	139.10(6)
S1-O2-Sr1a	142.9(1)
C5-O8-Sr1	125.4(1)
S1-O1-Sr1	146.9(1)
C4-O7-Sr1	120.6(1)
O7-Sr-O8	57.19(5)
C5-C4-O7-Sr1	14.3(3)
O8-Sr1-O7-C4	– 14.5(2)
C4-C5-O8-Sr1	– 14.7(3)
O7-Sr1-O8-C5	15.0(2)

[a] The equivalent positions for $P\bar{1}$ are 1) x,y,z and 2) $-x,-y,-z$.

ligands (Figure 9). The distances between columns are less than in the Ca^{2+} network, with Sr–Sr distances measuring 9.41 Å in the *y* direction, and 8.23 Å along the *z* direction. The sheets lie in the *ab* plane with a *d* spacing of 10.6 Å. The coordinated water molecules mostly occupy the interlayer region. The layers are held together by a network of hydrogen bonds between coordinated water molecules (D···A 2.773(3) – 3.135(3) Å), while three hydrogen bonds bind guest water to the framework (D···A 2.650(3) – 2.900(3) Å).

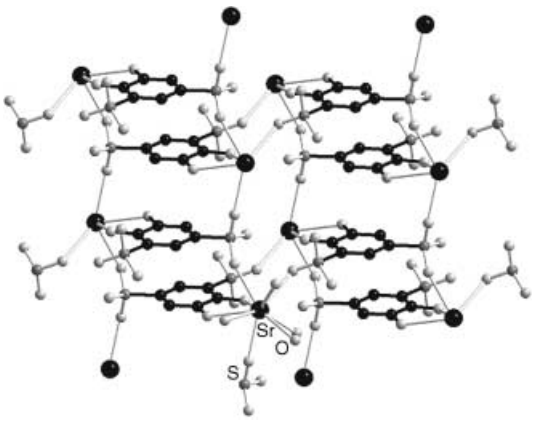

Figure 9. The 2D layer in $[Sr(L)(H_2O)_4]\cdot H_2O$ formed by the cross linking the 1D chain motif observed in the Ca structure (Figure 8). For all but the labeled Sr center, coordinated H_2O molecules have been omitted for clarity.

$[Ba(L)(H_2O)]\cdot H_2O$ (4): The columnar motif is lost in the Ba^{2+} network, giving way to a microporous pillared layered structure (Figure 5). The structure consists of layers of sulfonate-bridged Ba^{2+} centers, in the *ab* plane (Figure 10) pillared by the 1,3-sulfonate substituted phenyl rings. Again chelation by the catechol moiety of L to Ba^{2+} center present is observed (Ba1 – O7 2.843(3), Ba1 – O8 2.791(3) Å). This chelation orients the sulfonate groups relative to the layers.

Table 4. Selected bond lengths [Å], angles [°] and torsion plane angles [°] for $[Ba(\boldsymbol{L})(H_2O)]\cdot H_2O$.

Ba1–O1	2.737(3)
Ba1–O2	2.875(3)
Ba1a–O5	2.750(3)
Ba1–O7	2.843(3)
Ba1–O9	2.751(3)
Ba1–O1a	3.002(3)
Ba1–O3	2.765(3)
Ba1a–O6	2.765(3)
Ba1–O8	2.791(3)
S1-O1-Ba1	97.8(1)
O1-Ba1-O2	48.0(1)
S2-O5-Ba1b	161.6(1)
C4-O7-Ba1	125.8(2)
O7-Ba1-O8	54.66(8)
S1-O2-Ba1	103.7(2)
Ba1-O1-Ba1a	114.9(1)
S2-O6-Ba1c	132.8(2)
C5-O8-Ba1	127.1(2)
C5-C4-O7-Ba1	8.8(5)
O8-Ba1-O7-C4	6.1(4)
C4-C5-O8-Ba1	– 1.1(5)
O7-Ba1-O8-C5	– 2.5(3)

[a] The equivalent positions for $P\bar{1}$ are 1) x,y,z and 2) $-x,-y,-z$.

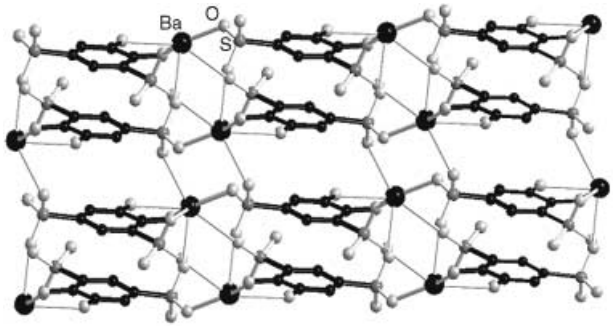

Figure 10. Aggregation pattern within the layer structure in $[Ba(L)(H_2O)]\cdot H_2O$. Coordinated H_2O molecules have been omitted for clarity.

Each Ba^{2+} is nine coordinate (cf. seven in **2** and eight in **3**) with an irregular geometry, and a coordination sphere composed of six sulfonate oxygen atoms, from five different sulfonate groups, the catechol oxygen atoms, and a water molecule (Ba1 – O9 2.751(3) Å) that projects into the interlayer. The construction of the layers is complex. Each molecule of L coordinates to six different Ba^{2+} centers. For L, in addition to the catechol chelation, the sulfonate group in the 3-position coordinates to two different Ba^{2+} centers, which are part of the same layer as the catechol-chelated Ba^{2+}, via a μ^2,η^2- mode (Ba1 – O5 2.750(3) Å, Ba1 – O6 2.749(3) Å). Sulfonate groups in the 1-position adopt a μ^3,η^3-coordination mode where all three Ba^{2+} ions are in the adjacent layer to those coordinating to the sulfonate in the 3-position. Each Ba^{2+} centers is chelated by two of the sulfonate oxygen atoms resulting in four coordinating interactions in total (Ba1 – O1 2.737(3) Å, 3.002(3) Å, Ba1 – O2 2.875(3) Å, Ba1 – O3 2.765(3) Å).

The catechol chelation to Ba1 directs L as a pillar to bridge layers through the sulfonate groups in the 1,3-positions to give a *d* spacing of 9.24 Å.[21] The BaL pillars pack inefficiently and open up 16-membered rings in the interlayer bordered by the

1,3-sulfonate groups. The rings align to form channels, measuring approximately 4 Å in diameter, filled with water molecules. Significantly, protons of the channel water of **4** were readily located in the Fourier difference map during the crystallographic refinement. The location of hydrogen atoms on water molecules in X-ray structures, especially uncoordinated, is not typical due to their weak ability to scatter X-ray radiation. This is notable as it indicates that these guests are strongly ordered by hydrogen bonding (D···A: O8···O10 2.616(3), O10···O4 2.752(3), O10···O10* 2.930(3) Å). Furthermore, it may indicate preferences of the framework for molecules of that particular shape.

Straightforward methods were used to prepare all the networks of L. Polycrystalline forms of the Ca^{2+} and Sr^{2+} networks, **2** and **3**, were afforded in high yields by neutralizing the disulfonic acid form of H_2L with the appropriate alkaline earth hydroxide. This is a convenient approach as the only by-product from the reaction is H_2O, as opposed to a second binary salt. H_2L was obtained by passing a solution of the commercially available Na_2L salt through a cation exchange resin. Preparation of $[Mg(H_2O)_6]\cdot L\cdot 3H_2O$ (**1**); directly from $H_2L_{(aq)}$ was not possible. The product upon neutralization with $Mg(OH)_2$ was not amenable to recrystallization from H_2O owing to its very high solubility. Analytically pure MgL could be obtained as $[Mg(L)(MeOH)_4]$ when the crude product was recrystallized from methanol.[27] This salt could then be dissolved in H_2O followed by slow evaporation to form **1**. The Ba^{2+} network, **4**, can be made metathetically in excellent yield upon mixture of aqueous solutions of $BaCl_2$ and Na_2L. A pure microcrystalline phase precipitates rapidly from solution.

To summarize the structures, in **1**, no catechol ligation nor direct metal–sulfonate contacts are formed and a solvent separated hydrogen bonded structure results. Compounds **2**–**4** are catechol ligated. Additionally, in **2**, one -SO_3 group is able to coordinate and bridge Ca^{2+} centers into columns. The increased affinity of Sr^{2+} in **3** for softer bases draws a second -SO_3 group into its coordination sphere and cross-links the columns together. In the 3D Ba^{2+} structure, **4**, there is markedly lower level of hydration of the metal ion compared with the other polymers, decreased from four to one aquo ligand, and a doubling of metal–sulfonate contacts from three to six. The increasing polarizability and atomic radii for alkaline earth ions and summary of the connectivity of the structures formed by L are shown in Table 5.[28] The coordination numbers are six for Mg^{2+}, eight for Ca^{2+}, and nine for both the Sr^{2+} and Ba^{2+} structures with L.

Identifying strategies to control network structures is important for the design and synthesis of functional solids whose properties are inherent to their 1D, 2D, or 3D structure.[2c, 29–32] For s-block coordination networks, only recently have trends in dimensionality been studied. Li et al. have examined the structures of the Ca^{2+}, Sr^{2+}, and Ba^{2+} salts of 3,5-pyrazoledicarboxylic acid (H_3pdc) formed under solvothermal conditions at differing levels of pH.[33] With this ligand, the network dimensionality was increased by sequential deprotonation of the ligand at higher pH levels. Although increasing the coordination ability of H_3pdc was the primary driving force for structure direction, the ability of Sr^{2+} and Ba^{2+} cations to accommodate more interactions due to their large radii was noted. Fromm has investigated the polymeric structures formed by hydrated Ca^{2+} and Ba^{2+} polyether complexes as their iodide salts.[34] Here, hydrated polyether M^{2+} units are cross-linked by hydrogen bonds between coordinated water molecules and uncomplexed iodide ions. The authors concluded that the dimensionality of the polymer that formed was primarily related to the number of water molecules per cationic complex, which in turn, could be controlled by the denticity of the polyether ligand and the radii of the cation used. More specifically with sulfonate ions, Squatritto and Cai have studied the coordination behavior of mono-[15] and disulfonate[16] ligands with alkali and alkaline earth cations. From these works only lamellar structures were obtained. There was an increase in coordination ability of the sulfonate ligands with the increasing charge/radius ratio of the cation.

Gas sorption studies with $[Ba(L)(H_2O)]\cdot H_2O$, 4: The PXRD and elemental analysis of the "as synthesized" bulk form of **4** match those of the single crystal, indicating the same structure. Thermal gravimetric analysis of **4** revealed that two mass losses before decomposition at 420 °C. Guest water molecules are lost up to 110 °C, followed by a second gradual mass loss between 130 and 164 °C corresponding to the loss of the coordinated water. Significantly, the PXRD analysis of heated samples of the dihydrate showed that the framework remained intact after loss of the channel water molecules. Loss of the second water molecule results in a substantial, yet efficient, phase transition to a different structure as judged by the sharp line shapes in the PXRD pattern of the fully dehydrated network (Figure 11).[22] The original $[Ba(L)(H_2O)]\cdot H_2O$ phase can be regenerated by immersion of the fully dehydrated powder in a 1:20 H_2O:EtOH solution, in which the network is insoluble, for 4 h (Figure 11).[23]

Given that the framework of **4** was sustained after removal of the channel water, this partially desolvated state was tested for its ability to include other guests. The following series of gaseous potential substrates was tested: CO, Cl_2, CH_4, NH_3, CO_2, SO_2, O_2, and H_2S.[22] For these experiments, $[Ba(L)(H_2O)]$, **4** with channel water removed, was generated

Table 5. Atomic radii and polarizabilities for Group II elements and connectivity summary for M^{2+}**L** structures.

Alkaline earth atom	Atomic radius[a] [Å]	Polarizability[b] [10^{-24} cm^3]	Dimensionality of network formed with L	CN	Total no. SO_3 O atoms coordinated (no. different SO_3 groups linked)
Mg	1.60	10.6	0	6	0 (0)
Ca	1.97	22.8	1	8	2 (2)
Sr	2.15	27.6	2	9	3 (3)
Ba	2.17	39.7	3	9	6 (5)

[a] Radii are based on the shortest distances in the metal. [b] Calculated static average electric dipole polarizabilities for ground state atoms. D: dimensionality. CN: coordination number. Values in the last column are the number of oxygen contacts to M^{2+} from -SO_3 groups; numbers in parentheses indicate the number of contacts to different -SO_3 groups.

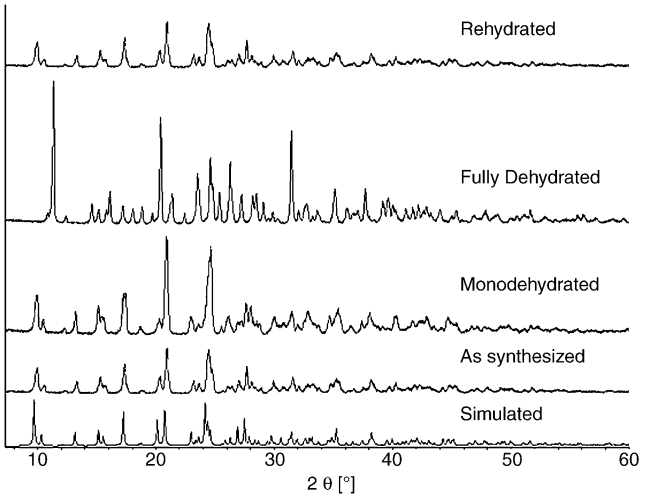

Figure 11. Powder X-ray diffraction patterns for the different phases of dehydrated forms and resolvated **4**.

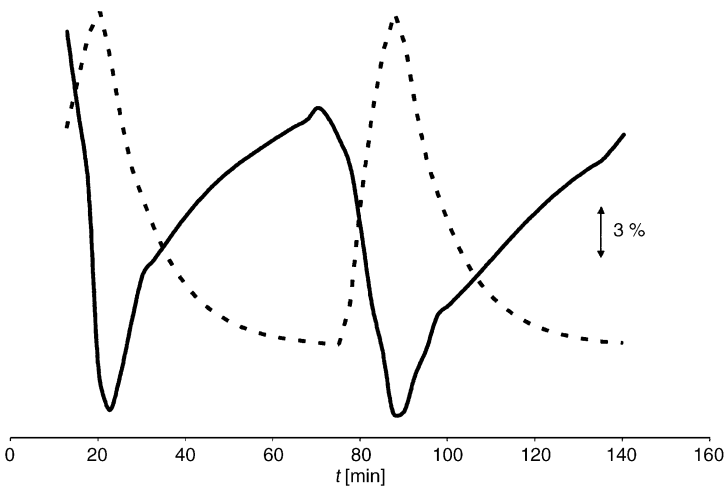

Figure 12. Temperature and thermogram curves for two cycles of sorption/desorption of H_2O in **4**. Solid line = mass profile; broken line = temperature profile.

in situ using the thermobalance, followed by changing the oven atmosphere from N_2 to the substrate gas. An increase in sample mass was taken as evidence for guest uptake. With H_2S at 50 °C, a mass increase of 7.5 % was observed, corresponding to the uptake of 0.93 equivalents of H_2S with respect to the equivalent of expelled water.[10, 24] Additional evidence for the sorption of H_2S was obtained using a gravimetric analysis. A sample of $[Ba(L)(H_2O)]\cdot H_2S_x$ was prepared by mono-dehydrating **4** in a N_2 purged flask, followed by H_2S purging. After removing excess H_2S, the sample was dissolved in 1M $Pb(NO_3)_2$.[25] A highly insoluble black PbS precipitate formed instantaneously, indicating H_2S in the sample. Quantification of the precipitate showed 0.62 equivalents of H_2S were included by $[Ba(L)(H_2O)]$.[25–26] A lower measured capacity by this method than by the thermobalance is to be expected due to loss of H_2S during sample handling. Significantly, no other guests showed any uptake, implying selectivity for H_2S.

The ability of $[Ba(L)(H_2O)]$ to resorb water vapor to regenerate **4** was also studied using the same methodology for measuring H_2S uptake. The optimal reversibility was found by heating **4** to 90 °C followed by cooling and introduction of humid N_2 (Figure 12). This degree of heating only results in partial dehydration of the network (75 %). This was necessary to lower the statistical loss of the second molecule of water which leads to deactivation by forming [Ba(L)]. Reversion of the structure to the channel form, by replacing the coordinated water molecule from humid N_2, is a much slower process than the sorbing of channel water. Resorption of water was quantitative for 2 cycles of sorption/desorption but was lowered to 33 % after seven cycles.

Compound **4** represents a microporous solid with selective gas uptake features. We regard L as acting as a "bent pillar" for the layers that packs inefficiently and, therefore, generates porosity in the interlayer. A comparison with prototypical layered metal–phosphonate structures is useful at this point. With a linear diphosphonate ligand, the organic moieties of the phosphonate pack efficiently, rendering the layered network ineffectual with regard to guest inclusion. This circumstance can be, in part, remedied by using mixed phosphonate/phosphate systems were the pillar alternates with a smaller, non-pillaring phosphonate group (e.g. methyl phosphonate or phosphate), to generate porosity.[35] However, in addition to complicating the synthesis, this may result in a loss of structural regularity and greater pore size distribution.[36] Use of a "bent" pillar, offers a facile two component synthesis of an ordered network with regular pores.

The selectivity of this network for H_2O and H_2S suggests that the empty channels are imprinted with the shape of a water molecule. This is corroborated by the fact the hydrogen atoms on the uncoordinated channel water molecules were readily located in the X-ray structure of **4**, indicating very strong hydrogen bonding. This hydrogen bonding has a prominent role in the sorption properties of **4** as methane (CH_4), which has a similar van der Waals radius to H_2S, but does not have hydrogen bond donor/acceptor capabilities, is not absorbed by the network. Compounds exhibiting sorption selectivity of H_2S over CH_4 are attractive candidates for industrial separations. For example, materials for sour gas abatement are highly sought after in natural gas production[37] and for the polishing of methane feedstocks for proton exchange membrane fuel cells.[38] Other examples of solid materials capable of H_2S uptake include micro- and mesoporous activated carbons,[39] cation exchanged zeolites,[40] and uncalcined and calcined limestone.[41]

The formation of the Ba^{2+} network, **4**, demonstrates the potential for preparing functional network solids from the assembly of coordinatively adaptable metals and ligands. Compound **4** is thermally stable to >400 °C and also towards reversible gas sorption. Another consideration is the synthesis of **4**, which is a highly efficient metathetical reaction. Compound **4** is prepared simply by combining equimolar aqueous solutions of Na_2L and $BaCl_2$, to spontaneously form a phase pure, microcrystalline precipitate in 93 % yield. Efficient metathesis reactions such as this indicate a strong thermodynamic driving force for the components towards a single structure. This is germane to the utility of sulfonates in the assembly of extended solids. Given that the instantaneous interactions that exist between Ba^{2+} and L in solution are

relatively weak and non-directional, these building blocks are able to rapidly adapt to one another to precipitate as a single, highly ordered phase rather than an amorphous compound.

Conclusion

With Group II cations, this study presents a strategy to form coordination networks not only with different levels of aggregation between metal ions and ligands, but also with different degrees of dimensionality. difference in the number of metal–sulfonate interactions that can form, as rationalized by hard–soft acid–base principles and cation radii, manifests into a dimensional evolution between the networks, progressing down the periodic family. In compound **4** there is a strong electronic correspondence between the chemically soft Ba^{2+} and L building blocks resulting in a highly cross-linked and stable structure results. This demonstrates that stable and functional coordination networks can be formed with organosulfonate ligands and soft closed shell cations. More generally, s-block cations should not be discounted as potential candidates for building blocks in extended coordination networks. Sulfonates represent an excellent choice of complementary ligand for these metals, where the variable coordination numbers and geometries of s-block cations are accommodated by the adaptive bonding capabilities of RSO_3 ligands.

Experimental Section

Materials and methods: All materials were obtained from Aldrich and used without further purification. Aqueous solutions of H_2L used to prepare the Mg^{2+}, Ca^{2+}, and Sr^{2+} salts were deoxygenated by sparging these solutions with nitrogen for 1 min to prevent oxidation of L. Once in the presence of a metal cation, L is stable in solution. All reported yields are isolated yields. Electrospray-ionization mass spectra (ESI-MS) were obtained using a Bruker Esquire 3000 spectrometer. Infrared spectra were obtained as KBr pellets on a Nicolet Nexus 470 Fourier transform spectrometer. Elemental analyses (C,H) were conducted by the Department of Chemistry Analytical Services at the University of Calgary. Powder XRD data was collected using a Rigaku Multiflex diffractometer operated using 0.02° step scan from 2–60° in 2θ and an exposure time of 1.0 s per degree.

General preparation of H_2L: ($[Na_2(L)(H_2O)]$) (1.00 g, 3.01 mmol) was dissolved in water (3 mL) and passed down a column containing Dowex 30×50 cation exchange resin (bed volume (BV) = 100 mL, 200 mesh) converted to the acid form by pretreatment with 1 BV of 6 N HCl. The H_2L was generated by eluting the column at a flow rate of ~ 3 mL min^{-1} and collecting a 40 mL fraction. The eluted solution was then directly treated with 3.01 mmol of the corresponding alkaline earth hydroxide and filtered.

Synthesis of $[Mg(L)(MeOH)_4]$: $Mg(OH)_2$ (0.174 g, 3.01 mmol) was added to an aqueous solution containing H_2L (3.01 mmol) and left to stir at room temperature for 6 h until all the $Mg(OH)_2$ had dissolved and the pH of the solution was >6. Evaporation of the solvent under reduced pressure resulted in a blue-black semi-solid of no definite composition. This residue was then taken up in MeOH (10 mL) with heating, cooled to 4 °C and filtered. To this solution Et_2O/MeOH 20:1 (20 mL) was added to precipitate a white polycrystalline powder that was then isolated by filtration. FT-IR (KBr): ν = 3415.4(br), 2361.2(s), 2333.8(s), 1651.0(s), 1481.l(s), 1181.2(br), 1104.7(s), 1033.7(s), 946.3(m), 858.2(m), 656.8(s), 596.7(s) cm^{-1}; DSC/TGA: 104–130 °C (408 J g^{-1}, endo) −28.6 % obsd, −30.4 % calcd for loss of 4 MeOH, 339.4 °C decomposition of L; yield: 0.840 g, 79 %; elemental analysis (%) calcd for: $Mg(C_6H_4O_8S_2)(MeOH)_4$: C 28.57, H 4.80; found: C 20.94, H 3.54.

Synthesis of $[Mg(H_2O)_6]\cdot L\cdot 3H_2O$ (1): In a minimum amount of water $[MgL(MeOH)_4]$ (0.250 g, 0.708 mmol) was dissolved and left to evaporate at room temperature to yield a white polycrystalline precipitate. FT-IR (KBr): ν = 3420.9(br), 2361.2(w), 2328.4(w), 1645.2(m), 1481.6(m), 1481.6(m), 1421.6(m), 1186.7(s), 1099.2(s), 1044.6(s), 946.3(w), 858.9(w), 755.1(w), 738.7(w), 667.7(m), 596.7(m) cm^{-1}; DSC/TGA: 78–102 °C (158.6 J g^{-1}, endo) −10.5 % obsd, −11.2 for loss of 2.5 H_2O; 122–155 °C (155.4 J g^{-1}, endo) −15.1 % obsd, −15.8 % for loss of 3.5 H_2O; 344 °C decomposition of L; yield: 0.301 g, 94 %; elemental analysis (%) calcd for: $Mg(C_6H_4O_8S_2)(H_2O)_6$: C 17.99, H 4.03; found: C 17.92, H 4.03. Single block shaped single crystals were selected from this solution at an intermediate stage of drying.

Synthesis of $[Ca(L)(H_2O)_4]\cdot H_2O$ (2): $Ca(OH)_2$ (0.223 g, 3.01 mmol) was added to an aqueous solution containing H_2L (3.01 mmol) and stirred at room temperature for 1 h until all $Ca(OH)_2$ and dissolved and the pH of the solution was >6. The water was removed under reduced pressure and the resulting residue redissolved in the minimum amount of water. Addition of an equal volume of a 1:1 solution of *i*PrOH and EtOH followed by cooling to 4 °C precipitated the product as a polycrystalline white solid, which was filtered off and washed with MeOH (3×5 mL). Yield: 1.01 g, 85 %; FT-IR (KBr): ν = 3546.6(br), 3464.6(br), 3071.3(br), 2710.8(br), 2361.2(w), 2333.8(w), 1623.7(m), 1394.2(m), 1285.0(s), 1197.6(br), 1104.7(s), 1071.9(s), 1030.1(s), 858.9(w), 755.1(w), 667.7(m), 602.1(s), 563.9(w), 520.2(w) cm^{-1}; DSC/TGA: 81–91 °C (232 J g^{-1}, endo) −9.24 % obsd, −9.97 % calcd for loss of 2 H_2O; 195–233 °C (248 J g^{-1}, endo) −4.96 % obsd, −4.99 % calcd for loss of 1 H_2O, 402 °C decomposition of L; elemental analysis (%) calcd for: $Ca(C_6H_4O_8S_2)(H_2O)_3$: C 19.89, H 2.78, found: C 20.94, H 1.71. Single crystalline material, obtained as plate-like crystals, was generated from vapor diffusion of EtOH into an aqueous solution of the product.

Synthesis of $[Sr(L)(H_2O)_4]\cdot H_2O$ (3): This compound was obtained analogously to the Ca salt for both the bulk material and single crystals using $Sr(OH)_2$ (0.366 g, 3.01 mmol). Yield: 1.10 g, 80.3 %. FT-IR (KBr): ν = 3563.0(br), 3218.8(br), 3071.3(br), 2732.6(w), 2355.7(w), 2333.8(w), 1640.1(w), 1585.4(w), 1448.7(w), 1377.9(w), 1285.0(m), 1225.0(s), 1192.1(s), 1099.1(s), 1044.6(s), 886.2(w), 858.9(w), 755.1(w), 651.3(m), 602.1(s), 558.4(w) cm^{-1}; DSC/TGA: 47–72 °C (221 J g^{-1}, endo) −12.0 % obsd, 12.1 % calcd for loss of 3 H_2O; 81.9–154.6 °C (51.3 J g^{-1}, endo) −4.2 % obsd, −4.0 % calcd for loss of 1 H_2O; 158–185 °C (104 J g^{-1}, endo) −3.75 % obsd, −4.0 % calcd for loss of 1 H_2O; 396 °C decomposition of L; elemental analysis (%) calcd for: $Sr(C_6H_4O_8S_2)(H_2O)_2$: C 18.39, H 2.05; found: C 18.32, H 1.91.

Synthesis of $[Ba(L)(H_2O)]\cdot H_2O$ (4):[10] $[Na_2(L)(H_2O)]$ (1.00 g, 3.01 mmol) was dissolved in a minimum amount of water and a saturated solution of $BaCl_2\cdot 2H_2O$ (0.735 g, 3.01 mmol) was added instantly forming a white polycrystalline powder that was filtered off and washed with MeOH (3×5 mL). Yield: 1.43 g, 93 %. FT-IR (KBr): ν = 3462.5(br), 3065.9(w), 2355.7(w), 2333.8(w), 1645.6(w), 1490.3(w), 1436.7(w), 1286.8(m), 1210.6(s), 1179.1(s), 1103.1(m), 1042.2(s), 886.2(w), 858.9(w), 755.1(w), 654.9(w), 604.6(m), 553.0(w), 536.6(w) cm^{-1}; DSC/TGA: 67–98 °C (35.2 J g^{-1}, endo) −3.60 % obsd, −4.08 % calcd for loss 1 H_2O; 130–164 °C (30.7 J g^{-1}, endo) −3.85 % obsd, −4.08 % calcd for loss 1 H_2O; 415 °C decomposition of L; elemental analysis (%) calcd for: $Ba(C_6H_4O_8S_2)(H_2O)_2$: C 16.25, H 1.63; found: C 16.32, H 1.83. Single crystals were obtained by the vapor diffusion of acetone into a saturated aqueous solution of the product.

Powder X-ray diffraction: The precipitate from the bulk syntheses of **4** was used as the "as synthesized" sample. The sample was prepared at different stages of solvation by heating in an oven just prior to analysis in accord with TGA measurements. All data were collected at room temperature in air using Al sample trays. No background corrections were applied to the data. An external calibration check was performed to assure proper alignment of the instrument.

General X-ray crystallography: Single crystal X-ray data for **1** and **2** were collected on a Nonius Kappa CCD diffractometer, for **3** and **4** on a Bruker SMART 1000 diffractometer. For all data sets, empirical absorption corrections were made using corrections routines associated with the respective instruments. The structures were solved using direct methods, refined, and hydrogen atoms located from Fourier difference maps for water molecules where possible, and constrained to maintain normal bond

lengths and angles, while all other hydrogen atoms were generated as riding spheres to their parent atoms, using the SHELXTL 97 suite of programs.[43]

CCDC-213065 (**1**), -213063 (**2**), -213064 (**3**) and -158325 (**4**) contain the supplementary crystallographic data for this paper. These data can be obtained free of charge via www.ccdc.cam.ac.uk/conts/retrieving.html, or from the Cambridge Crystallographic Data Centre, 12 Union Road, Cambridge CB2 1EZ, UK; fax: (+44)1223–336033; or email: deposit@ccdc.cam.ac.uk.

Thermogravimetric analysis procedures: Thermogravimetric analysis (TGA) and differential scanning calorimetry (DSC) were performed on a Netzsch 449C Simultaneous Thermal Analyzer with Al sample pan and an empty Al pan, as reference. The dynamic heating programs were conducted with a constant flow of dried ($CaCl_2$) N_2 being maintained. For gas sorption experiments, the apo-host was generated in situ with the thermal analyzer via a dynamic heating program (10 K min^{-1} to 90 or 110 °C) followed by an isothermal time at peak temperature for 1 min. The heating was then ceased and the instrument allowed to cool to ambient temperature. At this time also, the oven atmosphere was switched to a mixture of the substrate gas and N_2 in a 15:1 *v*/*v* ratio. The uptake of the gas, was evidenced by an increase in the observed mass and recorded as a function of time. All substrate gasses were dehydrated according to standard procedures.[43] For water uptake experiments, humidified N_2 gas was introduced by allowing a portion (93%) of the nitrogen feed to the instrument to pass over a ca. 12 cm^2 pool of water at flow rate of 40 mL min^{-1}. All temperature programs were run in the absence of sample and this data subtracted from samples to correct for effects of the instrument and for changes in buoyancy from the introduction of different atmospheres and temperatures.

Identification of H_2S in 4: A sample $[Ba(L)(H_2O)]\cdot H_2O$ (0.250 g, 0.566 mmol) in a nitrogen purged round bottom flask was subjected to a temperature program required to generate $[Ba(L)(H_2O)]$, compound **4** with channel H_2O removed. Subsequently, the flask was purged, then pressurized to 1.34 atm (5 psi) for 1 min with H_2S, and again purged with nitrogen to remove excess H_2S. This material was then removed from the flask then dissolved in a 1 mol L^{-1} aqueous solution of $Pb(NO_3)_2$ (15 mL). Observation of the highly insoluble black PbS precipitate was instantaneous. The solubility of the Ba salt is markedly enhanced in aqueous 1 mol L^{-1} $Pb(NO_3)_2$ due to the presence of a large excess of cations driving complex ion formation.

Acknowledgement

We thank the Natural Sciences and Engineering Research Council (NSERC) of Canada for funding and postgraduate scholarship to APC. We also thank Drs. Gary Enright and John Ripmeester at the Steacie Institute for Molecular Sciences, NRCC for use of their PXRD, and Dr. Robert McDonald (University of Alberta) for collection of the single crystal X-ray data for **3** and **4**. The efforts of Ms. Heather Reader and Dr. Kevin Thurbide (University of Calgary) in studying the chromatographic properties of **4** are also appreciated.

[1] T. J. Barton, L. M. Bull, W. G. Klemperer, D. A. Loy, B. Mc Enaney, M. Misono, P. A. Monson, G. Pex, G. W. Schere, J. C. Vartuli, O. M. Yaghi, *Chem. Mater.* **1999**, *11*, 2633.

[2] For reviews on crystal engineering see: a) M. D. Hollingsworth, *Science* **2002**, *295*, 2410; b) B. Moulton, M. J. Zaworotko, *Chem. Rev.* **2001**, *101*, 1629; c) P. J. Hagrman, D. Hagrman, J. Zubieta, *Angew. Chem.* **1999**, *111*, 2798; *Angew. Chem. Int. Ed.* **1999**, *38*, 2639; d) M. Eddaoudi, D. B. Moler, H. L. Li, B. L. Chen, T. M. Reineke, M. O'Keeffe, O. M. Yaghi, *Acc. Chem. Res.* **2001**, *34*, 319; e) O. M. Yaghi, H. L. Li, C. Davis, D. Richardson, T. L. Groy, *Acc. Chem. Res.* **1998**, *31*, 474.

[3] Selected recent examples of functional coordination networks, carboxylates: a) M. Eddaoudi, J. Kim, N. Rosi, D. Vodak, J. Wacher, M. O'Keefe, O. M. Yaghi, *Science* **2002**, *295*, 469; b) M. Eddaoudi, J. Kim, M. O'Keefe, O. M. Yaghi, *J. Am. Chem. Soc.* **2002**, *124*, 376; c) H. L. Li, J. Kim, T. L. Groy, M. O'Keeffe, O. M. Yaghi, *J. Am. Chem. Soc.* **2001**, *123*, 4867; d) S. S. Y. Chui, S. M. F. Lo, J. P. H. Charmant, A. G. Orpen, I. D. Williams, *Science* **1999**, *283*, 1148; pyridines: e) G. J. Harder, C. J. Kepert, Moubaraki, K. S. Murray, J. D. Cashion, *Science* **2002**, *298*, 1762; f) K. Biradha, M. Fujita, *Angew. Chem.* **2002**, *114*, 3542; *Angew. Chem. Int. Ed.* **2002**, *41*, 3392; g) K. Biradha, Y. Hongo, M. Fujita, *Angew. Chem.* **2002**, *114*, 3545; *Angew. Chem. Int. Ed.* **2002**, *41*, 3395, and references therein.

[4] a) O. D. Friedrichs, M. O'Keeffe, O. M. Yaghi, *Acta Crystallogr.* **2003**, *A59*, 22; b) R. Robson, *J. Chem. Soc. Dalton Trans.* **2000**, 3735; c) M. O'Keefe, M. Eddaoudi, H. L. Li, T. Reineke, O. M. Yaghi, *J. Solid State Chem.* **2000**, *152*, 3.

[5] Examples of coordination polymers formed from Group 2A cations: Carboxylates: a) I. R. Amiraslanov, V. N. Musaev, K. S. Marmedov, *Zh. Strukt. Khim.* **1982**, *23*, 114; b) V. A. Uchtman, R. J. Jandacek, *Inorg. Chem.* **1980**, *19*, 350; c) R. H. Groeneman, J. L. Atwood, *Cryst. Eng.* **1999**, *2*, 241; d) T. C. W. Mak, Y. Wai-Hing, G. Smith, E. J. O'Reilly, C. H. L. Kennard, *Inorg. Chim. Acta* **1987**, *88*, 35; e) L. R. Nassimbeni, S. Hong, *J. Chem. Soc. Dalton Trans.* **2000**, 349; f) M. J. Plater, A. J. Roberts, J. Marr, E. E. Lachowski, R. A. Howie, *J. Chem. Soc. Dalton Trans.* **1998**, 797; g) R. Murugavel, K. Baheti, G. Anantharaman, *Inorg. Chem.* **2001**, *40*, 6870; phosphonates: h) G. W. Svetich, C. N. Caughlan, *Acta Crystallogr.* **1963**, *A16*, 73; i) K. J. Langley, P. J. Squattrito, F. Adani, E. Montoneri, *Inorg. Chim. Acta* **1994**, *253*, 77; j) D. M. Poojary, G. Zhang, A. Cabeza, M. A. G. Aranda, S. Bruque, A. Clearfield, *J. Mater. Chem.* **1996**, *6*, 639; other ligands: k) J. M. Harrowfield, R. P. Sharma, B. W. Skelton, Venugopalam, A. H. White, *Aust. J. Chem.* **1998**, *51*, 775; l) C. Robi, *Z. Naturforsch. Teil B.* **1987**, *42*, 972; m) R. Murugavel, V. V. Karambelkar, G. Anantharaman, M. G. Walawalkar, *Inorg. Chem.* **2000**, *39*, 1381; n) J. A. Kanters, W. J. J. Smeets, A. J. M. Disenberg, K. Venkatasubramanian, N. S. Poonia, *Acta Crystallogr.* **1984**, *C40*, 1699.

[6] For a reviews on the coordination chemistry of alkali and alkaline earth cations see: a) N. S. Poonia, A. V. Bajaj, *Chem. Rev.* **1979**, *79*, 389; b) D. E. Fenton in *Comprehensive Coordination Chemistry*, *Vol. 3* (Eds.: S. Wilkinson, R. D. Gillard, J. A. McCleverty), Pergamon, Oxford, **1987**, p. 1.

[7] For reviews see: a) A. Clearfield, *Prog. Inorg. Chem.* **1998**, *47*, 371; b) G. Alberti, in *Comprehensive Supramolecular Chemistry*, *Vol. 7* (Eds.: J. L. Atwood, J. E. Davies, D. D. MacNicol, F. Vögtle), Pergamon, Oxford, **1996**, p. 151.

[8] Charge assisted hydrogen bonding between aqua-metal ions and sulfonate anions has been studied as a means to construct infinite frameworks, see a) S. A. Dalrymple, M. Parvez, G. K. H. Shimizu, *Inorg. Chem.* **2002**, *41*, 6986; b) S. A. Dalrymple, G. K. H. Shimizu, *Chem. Commun.* **2002**, 2224; c) D. S. Reddy, S. Duncan, G. K. H. Shimizu, *Angew. Chem.* **2003**, *115*, 1398; *Angew. Chem. Int. Ed.* **2003**, *42*, 1360; d) J. L. Atwood, J. W. Steed, C. B. Bauer, R. D. Rogers, *Inorg. Chem.* **1996**, *35*, 2602; e) A. J. Shubnell, E. J. Dosnic, E. L. McClymont, P. J. Squattrito, *Inorg. Chim. Acta* **1992**, *201*, 143; f) M. A. Leopard, P. J. Squattrito, S. N. Dubey, *Acta Crystallogr.* **1999**, *C55*, 35.

[9] a) S. K. Makinen, N. J. Melcer, M. Parvez, G. K. H. Shimizu, *Chem. Eur. J.* **2001**, 7, 5176; b) A. P. Côté, M. J. Ferguson, K. A. Kahn, G. D. Enright, A. D. Kulynych, S. A. Dalrymple, G. K. H. Shimizu, *Inorg. Chem.* **2002**, *41*, 287; c) B. D. Chandler, A. P. Côté, D. T. Cramb, J. M. Hill, G. K. H. Shimizu, *Chem. Commun.* **2002**, 1900.

[10] A. P. Côté, G. K. H. Shimizu, *Chem. Commun.* **2001**, 251.

[11] The supramolecular chemistry of sulfonated calixarenes with hydrated lanthanide and other cations have been explored by Atwood and Raston. These inclusion compounds can form extended structures in the solid-state. See: a) J. L. Atwood, L. J. Barbour, S. J. Dagarno, C. L. Raston, H. R. Webb, *J. Chem. Soc. Dalton Trans.* **2002**, 4351; b) S. J. Dagarno, C. L. Raston, *Chem. Commun.*, **2002**, 2216; c) J. L. Atwood, L. J. Barbour, M. J. Hardie, C. L. Raston, *Coord. Chem. Rev.* **2001**, *222*, 3; d) H. R. Webb, M. J. Hardie, C. L. Raston, *Chem. Eur. J.* **2001**, *7*, 3616.

[12] A. P. Côté, G. K. H. Shimizu, *Coord. Chem. Rev.* in press.

[13] For example, a minor change from Ag benzenesulfonate to *p*-toluenesulfonate alters the bridging mode of the SO_3 group from μ^6 to μ^5, see: a) G. K. H. Shimizu, G. D. Enright, K. F. Preston, C. I. Ratcliffe, J. L. Reid, J. A. Ripmeester, *Chem. Commun.* **1999**, 1485; b) G. K. H. Shimizu, G. D. Enright, C. I. Ratcliffe, G. S. Rego, J. L. Reid, J. A. Ripmeester, *Chem. Mater.* **1998**, *47*, 371. Also see: c) J. O. Yu, A. P. Côté, G. D. Enright, G. K. H. Shimizu, *Inorg. Chem.* **2001**, *40*, 582.

[14] J.-M. Lehn, *Supramolecular Chemistry-Concepts and Perspectives*, Wiley-VCH, Weinheim **1995**.

[15] A. J. Shubnell, E. J. Kosnic, P. J. Squattrito, *Inorg. Chim. Acta* **1994**, *216*, 101.

[16] J. Cai, C.-H. Chen, C.-Z. Liao, X.-L. Feng, X.-M. Chen, *Acta Crystallogr.* **2001**, *B57*, 520.

[17] Compound **4** and preliminary gas uptake results has been the subject of an earlier communication. See ref. [10].

[18] 4,5-Dihydroxybenzene-1,3-disulfonate is used as a complexometric indicator (commercially known as Tiron) for divalent transition metal ions via 4,5-diol chelation, see: a) S. Abe, T. Saito, M. Suda, *Anal. Chim. Acta* **1986**, *181*, 203; b) Z. Zhang, R. B. Jordan, *Inorg. Chem.* **1996**, *35*, 1571, and references therein. For the Ca^{2+}, Sr^{2+}, and Ba^{2+} salts, the formation of the chelated discrete complex in solution is evidenced by observation of the corresponding molecular ions in ESI-MS spectra. ESI-MS (*m*/*z*): M^- $(CaL)^- = 307.15$; M^{2-} $(CaLH_2O)^{2-} = 187.85$; $(BaLH)^+ = 406.85$.

[19] Solvento Mg^{2+} sulfonates: a) V. Cody, J. Hazel, *Acta Crystallogr.* **1977**, *B33*, 3180; b) J. M. Broomhead, A. D. I. Nicol, *Acta Crystallogr.* **1948**, *1*, 88; c) J.-J. Wang, L. Bo, F.-M. Mioao, *Chin. J. Struct. Chem.* **1994**, *13*, 304; d) V. Shakeri, S. Haussuhi, *Z. Kristallogr.* **1992**, *198*, 169; e) W. H. Ojala, L. K. Lu, K. E. Albers, W. B. Gleason, T. I. Richardson, R. E. Louvrien, E. A Sudbeck, *Acta Crystallogr.* **1994**, *B50*, 684.

[20] A detailed view of the hydrogen bonding in this compound is provided in the supplemental material. For a discussion on hydrogen bonding patterns between organosulfonates hexaaquo metal cations see refs. [8a] and [8b].

[21] The anchoring role of the catechol moiety is an important feature in this network. As a comparison, Ba(1,3-benzenedisulfonate) forms a dense 2D layered structure: A. P. Côté, G. K. H. Shimizu, unpublished results.

[22] Determination of the sorption of NH_3, which has a similar van der-Waals radius and hydrogen bonding potential as H_2O, was difficult owing to effects of our thermogravimetric apparatus that seems to also have an affinity for this gas. This made reliable measurement of mass changes not possible.

[23] $[BaL(H_2O)]$ has a mass of 423 $g\,mol^{-1}$. In terms of molar equivalents, a 7.5% mass gain is therefore equivalent to 31.68 $g\,mol^{-1}$ or 31.68/(34.06 $g\,mol^{-1}$ H_2S) = 0.93 equivalents of H_2S.

[24] The solubility of the Ba salt is markedly enhanced in aqueous 1 $mol\,L^{-1}$ $Pb(NO_3)_2$ due to the presence of a large excess of cations driving complex ion formation.

[25] 0.250 g $[Ba(L)(H_2O)]\cdot H_2O$/441.58 $g\,mol^{-1}$ $\rightarrow$ 0.566 mmol potential capacity for H_2S. Collected 0.083 g PbS/239.3 $g\,mol^{-1}$ = 0.351 mmol, after washing and drying. Therefore, the number of measured equivalents sorbed = 0.351 mmol/0.566 mmol = 0.62. A photograph showing the formation of PbS in this experiment is provided as supplemental material.

[26] G. Svehla, *Vogel's Handbook of Qualitative Inorganic Analysis*, 7th ed., Addison Wesley Longman, Essex, **1997**.

[27] Crystal data for $[Mg(L)(MeOH)_4]$: $C_{10}H_{19}O_{12}S_2Mg$, F_w = 419.68 $g\,mol^{-1}$, monoclinic, space group *C*2/*c*, $a = 13.734(5)$, $b = 7.503(5)$, $c = 16.916(5)$ Å, $b = 96.441(5)^\circ$, $V = 1732.1(14)$ Å^3; $Z = 4$, $\rho_{calcd} = 1.609$ $Mg\,m^{-3}$, $R = 0.0428$, $Rw = 0.1373$, and GOF = 1.148 for 126 parameters using 1956 ($F_o > 2.0\sigma(F_o)$) reflections. $Mo_{K\alpha}$ radiation ($\lambda = 0.71073$), $\mu(Mo_{K\alpha})$ 0.806 mm^{-1}. Please see Supporting Information for structural illustrations, further experimental information, and connectivity data.

[28] *CRC Handbook of Chemistry and Physics* (Ed.: R. C. Weast), 1st student ed., CRC Press Inc., Boca Raton, **1988**.

[29] a) D. Hagrman, R. P. Hammond, R. Haushalter, J. Zubieta, *Chem. Mater.* **1998**, *10*, 2091; b) D. J. Chesnut, D. Plewak, J. Zubieta, *J. Chem. Soc. Dalton Trans.* **2001**, 2567.

[30] a) S. Natarajan, *Inorg. Chem.* **2002**, *41*, 5530; b) K. H. Lii, Y. F. Huang, V. Zima, C. Y. Huang, H. M. Lin, Y. C. Jiang, F. L. Liao, S. L. Wang, *Chem. Mater.* **1998**, *10*, 2599.

[31] R. Vaidhyanathan, S. Natarajan, C. N. R. Rao, *Inorg. Chem.* **2002**, *41*, 5226.

[32] Y. Rodrigues-Martin, M. Hernández-Molina, F. S. Delgado, J. Pasán, C. Ruiz-Pérez, J. Sanchiz, F. Lloret, J. Julve, *Cryst. Eng. Commun.* **2002**, *4*, 522.

[33] L. Pan, T. Frydel, M. B. Sander, X. Huang, J. Li, *Inorg. Chem.* **2001**, *40*, 1271.

[34] a) K. M. Fromm, *Chimia* **2002**, *56*, 676; b) K. M. Fromm, *Chem. Eur. J.* **2001**, *7*, 2263.

[35] a) G. Alberti, U. Costantino, F. Marmottini, R. Vivani, P. Zappelli, *Angew. Chem.* **1993**, *105*, 1396; *Angew. Chem. Int. Ed. Engl.* **1993**, *32*, 1357; b) G. Alberti, F. Marmottini, S. Murcia-Mascarós, R. Vivani, *Angew. Chem.* **1994**, *106*, 1655; *Angew. Chem. Int. Ed. Engl.* **1994**, *33*, 1594; c) N. J. Clayden, *J. Chem. Soc. Dalton Trans.* **1987**, 1877.

[36] G. Alberti, U. Costantino, F. Marmottini, R. Vivani, P. Zappelli, *Mater. Res. Soc. Symp. Proc.* **1991**, 233, 101.

[37] For a lead reference see: D. Sanopoulos, A. Karabelas, *Energy Sources* **1997**, *19*, 63.

[38] a) I. Rossa, E. Garrone, F. Geobaldo, B. Onida, G. Saracco, V. Specchia, *Appl. Catal. B Environ.* **2001**, *34*, 29; b) Y. Matsuzakio, I. Yasuda, *Solid State Ionics* **2000**, *132*, 261.

[39] a) R. Yan, D. T. Liang, L. Tsen, J. H. Tay, *Environ. Sci. Technol.* **2002**, *36*, 4460; b) T. J. Bandosz, *Carbon* **1999**, *37*, 483; c) A. Turk, E. Sakalis, J. Lessuck, H. Karamitsoss, O. Rago, *Environ. Sci. Technol.* **1989**, 23, 1242.

[40] S. B. Jang, M. S. Jeong, Y. Kim, Y. W. Han, K. Seff, *Microporous Mesoporous Mater.* **1998**, *23*, 33.

[41] a) L. A. Fenouil, S. Lynn, *Ind. Eng. Chem. Res.* **1995**, *34*, 2324; b) L. A. Fenouil, S. Lynn, *Ind. Eng. Chem. Res.* **1995**, *34*, 2334.

[42] G. M. Sheldrick, *SHELX-97 Program for X-ray Crystal Structure Refinement*, University of Göttingen (Germany), **1997**.

[43] W. L. F. Armarego, D. D. Perrin, *Purification of Laboratory Chemicals*, 4th ed., Reed Education and Professional Publishing, Oxford, **1996**.

Received: May 5, 2003 [F5102]